PAPER

Check for updates

A role for terpenoid cyclization in the atom economical polymerization of terpenoids with sulfur to yield durable composites†

Charini P. Maladeniya, Menisha S. Karunarathna, Moira K. Lauer, Claudia V. Lopez, Timmy Thiounn and Rhett C. Smith ⓘ *

Renewably-sourced, recyclable materials that can replace or extend the service life of existing technologies are essential to accomplish humanity's quest for sustainable living. In this contribution, remeltable composites were prepared in a highly atom-economical reaction between plant-derived terpenoid alcohols (10 wt% citronellol, geraniol, or farnesol) and elemental sulfur (90 wt%). Investigation into the microstructures led to elucidation of a mechanism for terpenoid polyene cyclization initiated by sulfur-centered radicals. The formation of these cyclic structures contributes significantly to understanding the mechanical properties of the materials and the extent to which linear *versus* crosslinked network materials are formed. The terpenoid–sulfur composites can be thermally processed at low temperatures of 120 °C without loss of mechanical properties, and the farnesol–sulfur composite so processed exhibits compressive strength 70% higher than required of concrete for residential building. The terpenoid–sulfur composites also resist degradation by oxidizing acid under conditions that disintegrate many commercial composites and cements. In addition to being stronger and more chemically resistant than some commercial products, the terpenoid–sulfur composites can be used to improve the acid resistance of mineral-based Portland cement as well. These terpenoid–sulfur composites thus hold promise as elements of sustainable construction on their own or as additives to extend the operational life of existing technologies, while the cyclization behaviour could be an important contributor in other polymerizations of terpenoids.

Introduction

Terpenes and terpenoids are leading candidates to supplant petrochemical olefins in the ongoing quest towards a green economy.[2] Terpene derivatives are readily available from many plants, bacteria and algae sources and so can be produced anywhere in the world, an important consideration for resilient, socially responsible sustainability strategies. A wide range of composites employing terpenoid or derivative monomers have been explored for the preparation of polymers with the aim of elucidating renewably-sourced alternatives to petrochemical olefins.[2–4]
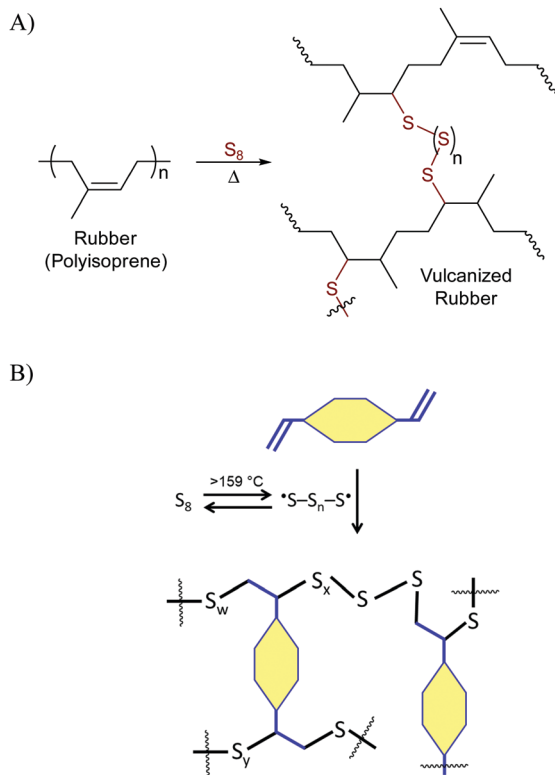
Organosulfur polymers and composites have attracted some attention as potentially robust and recyclable alternatives to petrochemical polyolefins as well. Sulfur is a surplus by-product removed from fossil fuels to prevent the release of sulfur combustion products into the atmosphere, so its valorisation

has attracted some interest. From a mechanistic standpoint, sulfur-induced crosslinking of olefins to access high sulfur-content materials relies on what has become known as inverse vulcanization.[5–8] Classic vulcanization was described by Charles Goodyear in 1844[9] as a process to strengthen natural rubber (polyisoprene) by its reaction with small quantities of sulfur (Scheme 1A). Inverse vulcanization relies on much of the same chemistry for crosslinking of olefins with sulfur, but in inverse vulcanization sulfur is often the majority component.[5–7,10] The general mechanism, initiated by the thermal generation of polymeric sulfur radicals from the S_8 allotrope, is shown in Scheme 1. It is notable that the inverse vulcanization process is theoretically 100% atom economical, though some loss of atoms in the form of H_2S is possible, a result of H-atom abstraction by sulfur-centred radicals. Materials made by inverse vulcanization can be durable polymers or composites in which polymeric sulfur domains, typically unstable at STP, are trapped and stabilized by the crosslinked network. Inverse vulcanization has proven successful for producing materials from a range of petrochemical and renewably-sourced olefins,[8] including terpenoids,[11–15] triglycerides,[16–23] fatty acids,[24–27] sorbitan esters,[28] amino acid derivatives,[29] guaiacol derivatives,[30] and

Department of Chemistry and Center for Optical Materials Science and Engineering Technologies, Clemson University, Clemson, South Carolina, USA.
E-mail: rhett@clemson.edu
† Electronic supplementary information (ESI) available. See DOI: 10.1039/d0ma00474j

A)

B)

Scheme 1 Simplified schemes for the Goodyear (A) and Pyun (B) variations of vulcanization processes.

Fig. 1 Schematic demonstrating plants from which terpenoids can be extracted for their polymerization with sulfur to give thermoplastics.

cellulose/lignin derivatives.[31–34] Many applications for resulting materials have been noted,[35,36] as highlighted in the aforementioned references. Significant advances in synthetic methodologies to allow lower-temperature/catalytic reactions[37–40] and facile processing[41,42] of high sulfur-content materials have recently made high sulfur content materials even more attractive candidates for commercialization.

The Smith group has recently explored strategies for preparing biomass-derived sulfur composites made from organic small molecules, traditional petrochemical composites, biocomposites, and amino acid-based monomers with a primary goal of developing durable structural materials.[25–27,29,31–34,43–45] These composites have shown mechanical strength profiles that in some cases outperform commercial building materials such as glass fibre-reinforced polymer composites or Portland cement. Unfortunately, some of these sulfur composites require several steps for monomer synthesis, detracting from the atom economy, greenness, and affordability of the processes.

The efficient formation of C–S bonds upon reaction of terpenes with sulfur radicals in the course of thiol–ene reactions has been established,[46,47] and a variety of terpenoids have been used as comonomers for reaction with sulfur by the inverse vulcanization pathway.[12,13] For the current study, it was thus hypothesized that terpenoid–sulfur composites (Fig. 1A) could themselves be structurally strong or that they could be used to improve the stability of mineral cements to oxidizing acid in a manner similar to prior work but without the need for synthetic modification of terpenoids prior to polymerization.
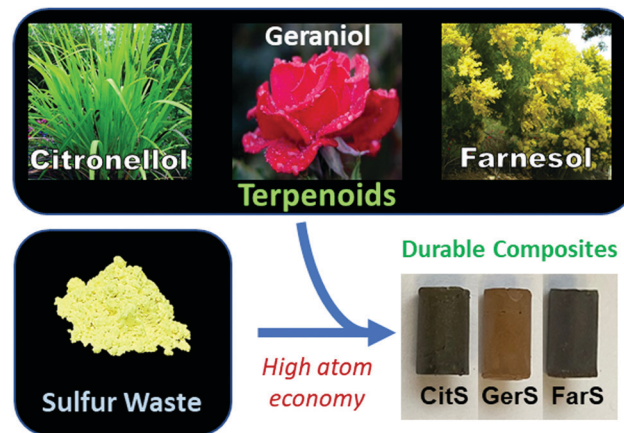
Despite rapidly-growing interest in high sulfur-content materials, an understanding of how monomer composition and sulfur:monomer ratio influence ultimate mechanical properties is still emerging, with the most comprehensive survey of this topic appearing quite recently.[48] Broadly, previous studies indicate that the crosslink density in olefin–sulfur composites plays an expectedly substantial role in the mechanical properties of the materials, so for the current study three terpenoids – citronellol, geraniol and farnesol – were selected for testing as examples of terpenoids having one, two or three olefin units per molecule, respectively. The density, water uptake, compressive strength and resilience to challenge by oxidizing acid were assessed for the terpenoid–sulfur composites. A role for the terpenoid–sulfur composites as low wt% additives to Portland cement was also investigated to assess whether their addition could protect cement from oxidizing acid challenge. In the course of this work, several cyclization mechanisms for geraniol and farnesol were identified that lead to the incorporation of cyclohexane derivatives into the polymer microstructures. Although such cyclic terpene derivatives are known in biology[49,50] and have been prepared in synthetic small molecule studies, such structures have generally not been invoked as microstructures of terpenoid-derived polymers.

Results and discussion

Synthesis and microstructure

Historically, citronellol, geraniol and farnesol were isolated from citronella grass, roses, and the farnese acacia trees, respectively.[51–54] Representative photos of these plants are provided in Fig. 1A. More recently, a variety of organisms have been engineered to more efficiently produce terpenoids,[55–59] and quite recently these approaches have been subject to promising techno-economic assessment of their viability to produce commodity terpenoids.[60,61] In the current case, sulfur–terpenoid composites were prepared by inverse vulcanization of elemental sulfur with 10 wt% of commercial citronellol, geraniol or farnesol to yield **CitS**, **GerS** or **FarS**, respectively to give materials initially hypothesized to have structures shown in Scheme 2.
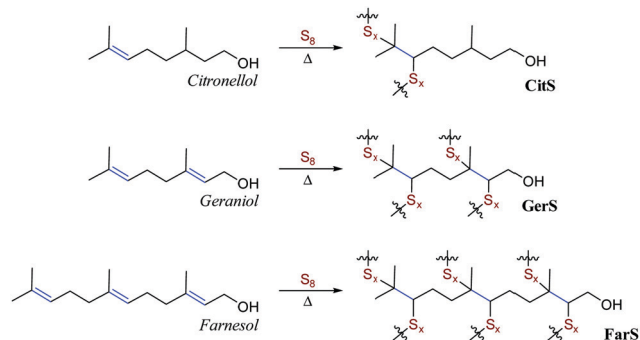
Scheme 2 Inverse vulcanization of terpenoid alcohols with elemental sulfur yields crosslinked composites **CitS**, **GerS** and **FarS**, shown with initially-hypothesized structures that would result from direct inverse vulcanization of individual olefin units.

Many of the aforementioned high sulfur-content materials comprising large percentages of sulfur are actually composites wherein the sulfur-crosslinked organic network is accompanied by sulfur (either polymeric or orthorhombic) that is not covalently attached to the network. This is the case for the terpenoid–sulfur materials in the current study as well. The relative amounts of free sulfur were determined by integration of the sulfur melting endotherm in the DSC traces for the composites (Fig. S5 and Table S1 in the ESI†). This analysis revealed noncovalent sulfur incorporation at a rate of 82, 57 and 56 wt% for **CitS**, **GerS** and **FarS**, respectively. The terpenoid–sulfur materials prepared herein are thus best described as composites made up of a sulfur-organic network and sulfur that is not covalently bound to the network.

The composites were brown, remeltable solids that could be readily fabricated into cylinders appropriate for compressive strength measurements by pouring molten samples into silicone moulds (Fig. 1 and Fig. S6, ESI†). While **FarS** exhibits the dark brown colour (thinner cross-sections appearing brown-orange) characteristic of many other inverse vulcanization products containing polymeric sulfur domains, **GerS** is notably lighter in colour. This lighter colour typically indicates the presence of high quantities of orthorhombic sulfur, which is yellow in colour. This observation was initially surprising given that diene geraniol lies between monoalkene citronellol and triene farnesol in terms of putatively crosslinkable olefins. Further analysis revealed that **GerS** also has a similar compressive strength (discussed in more detail in the following section) to that of **CitS**. Given that the mechanical strength of high sulfur-content materials generally increases with increasing crosslink density for comparable monomers, the similar compressive strengths of **CitS** and **GerS** suggested that they may have similar crosslink densities. In an effort to understand these observations, the crosslinking mechanism in geraniol–sulfur polymer **GerS** was investigated in greater detail.

In addition to simple olefin crosslinking by sulfur to give the initially-hypothesized structures shown in Scheme 2, another potential reaction pathway to consider is intramolecular cyclization (Scheme 3A). Such cyclization reactions are well-precedented for geraniol and can be facilitated enzymatically,[62] by zeolytes,[1] upon reaction with N-bromosuccinimide (NBS),[63] or with other
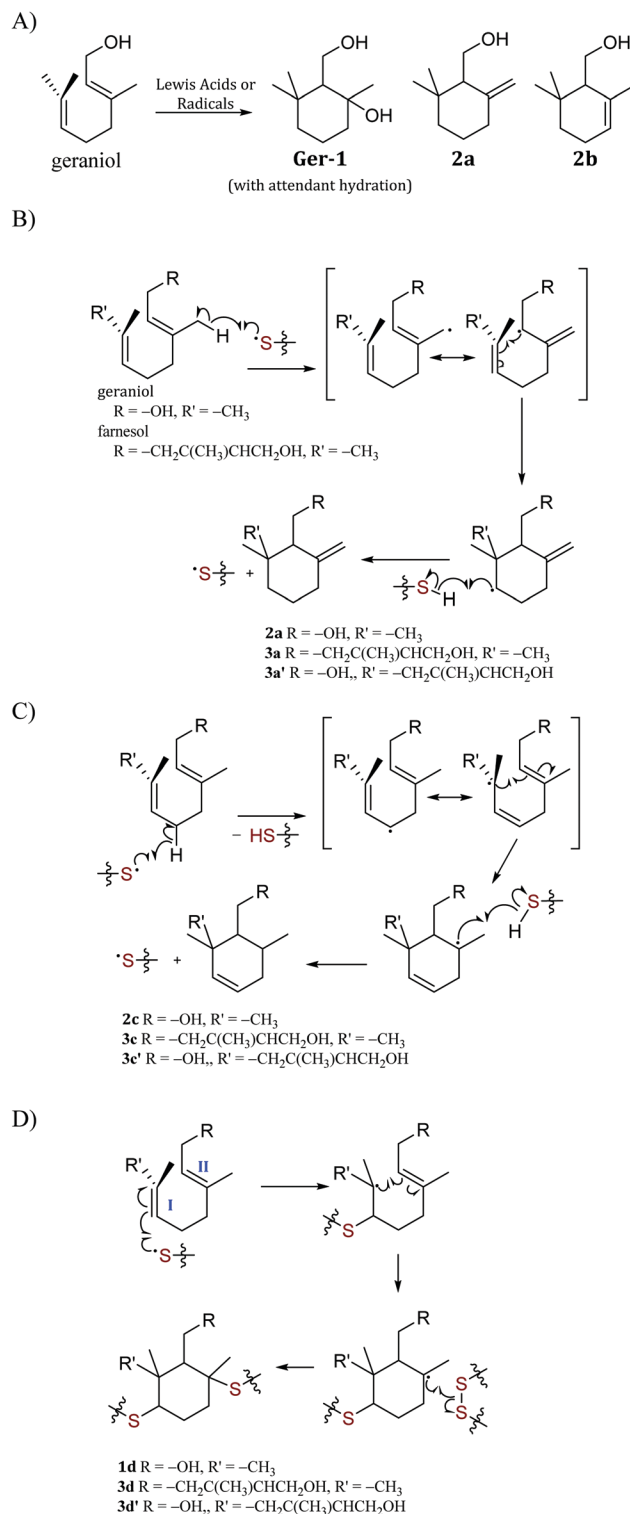
Scheme 3 Reported cyclization products of terpenoid polyenes (A), and mechanisms of sulfur radical-induced cyclization of geraniol or farnesol via initial H-atom abstraction (B) and (C) or addition across olefins (D).

oxidizing agents or Lewis acids.[64,65] Cyclization of geraniol to form known compounds **2a** and **2c** in the course of **GerS** synthesis could follow initial allylic H-atom abstraction from geraniol by thermally-generated sulfur radicals according
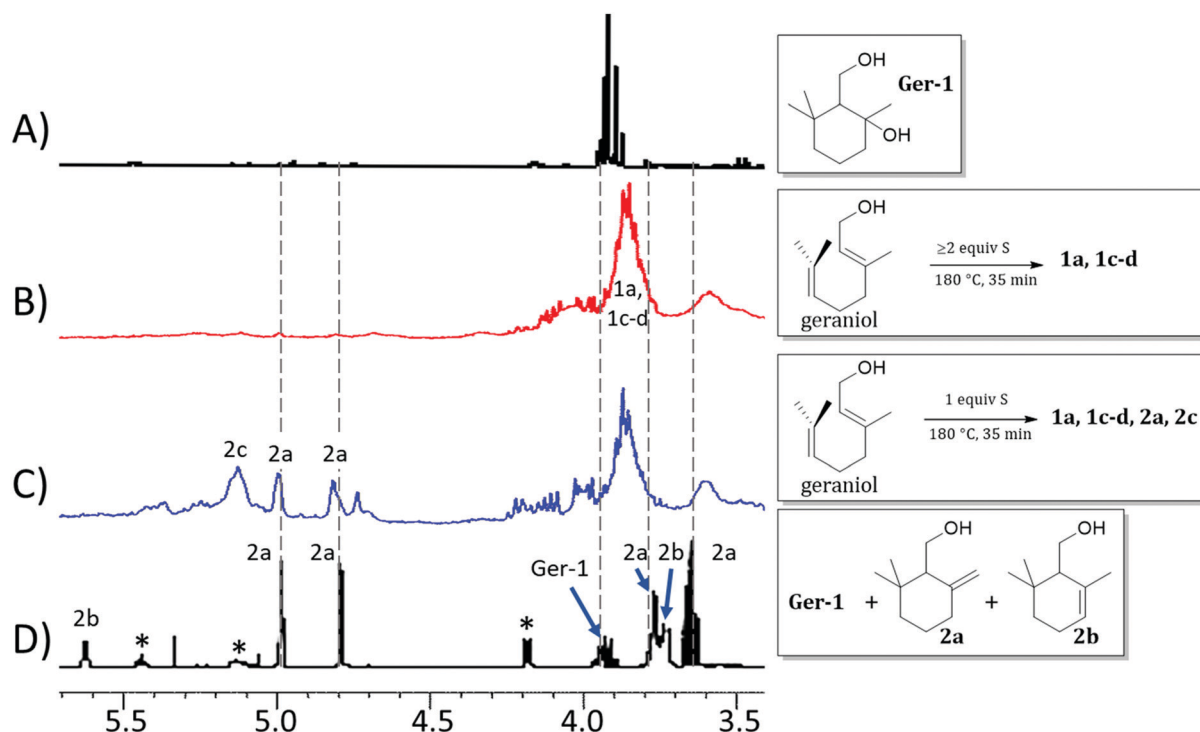
Fig. 2 Proton NMR spectra (CDCl₃, 300 MHz) for (A) isolated **Ger-1**, (B) product mixture resulting from the reaction of geraniol with ≥2 equiv. S, (C) product mixture resulting from the reaction of geraniol with 1 equiv. S, and (D) literature spectrum for a mixture of geraniol (peaks marked with asterisks), **2a** and **2b**. Spectra (A) and (D) are reprinted from reference[1] ©2005, with permission from John Wiley and Sons.

to mechanisms such as those shown in Scheme 3B and C. Additional mechanisms involving reaction of sulfur radical with the resultant olefins could also lead to saturated cyclic microstructures (Scheme 3D) similar to **Ger-1**. In Scheme 3D, initial attack of sulfur at either olefin I or II will both lead to formation of species **1d**, though only one of these possibilities is shown for illustration. Radicals shown to abstract H atoms from putative thiol moieties may alternatively react with poly-sulfur chains for direct C–S bond-formation.

Should formation of such cyclic products contribute significantly to the microstructure of **GerS**, its mechanical properties could be significantly influenced. In an effort to assess the possibility for the formation of cyclic structures during polymerization, the reaction of geraniol with 1–4 equivalents of sulfur was carried out under the conditions used to prepare **GerS** and the products of these reactions were analysed by ¹H NMR spectrometry (Fig. 2; summary of structures provided in Scheme 4 and Table 1). It was necessary to characterize these soluble products because **GerS** itself is not fully soluble.

When geraniol undergoes reaction with one equivalent of sulfur under conditions identical to those used to prepare **GerS**, the ¹H NMR spectrum of the product mixture (Fig. 2C) shows resonances attributable to known geraniol cyclization products **2a** and **2c**. A reported spectrum[1] for a product mixture containing geraniol, **2a** and **2b** (**2b** was not observed in the current case) is shown in Fig. 2D and a published spectrum[1] for isolated **Ger-1** is shown in Fig. 2A for comparison. In addition to **2a** and **2c**, resonances comparable to those for saturated species **Ger-1** were observed. In the current case, resonances in this

range may be attributed to analogous species **1a**, **1c** and **1d** (Scheme 4 and Table 1), the expected products of inverse vulcanization of the initially-formed cyclic olefins. The reso-nances for sulfur-derivatized **1a**, **1c** and **1d** are expectedly shifted upfield with respect to those for oxygen-substituted **Ger-1**.

The reaction of geraniol was similarly repeated with 2 or 4 equivalents of sulfur, and the ¹H NMR spectra for these two trials looked nearly identical (the spectrum for reaction with 4 equiv. S is shown in Fig. 2B). At this point, essentially all of the olefinic resonances have disappeared, consistent with their consumption upon crosslinking with sulfur by the anticipated inverse vulcaniza-tion reaction, leading to almost entirely saturated species **1**. On the basis of the ¹H NMR studies, it can be concluded that several additional sulfur-crosslinked microstructures beyond those shown in Scheme 2 are actually present in **GerS**, as delineated in Scheme 4.

In addition to the predominant species identified from the ¹H NMR spectra shown in Fig. 2, a very minor contribution (<2%) of aromatic species, previously reported to result from repetitive electron/hydrogen transfer processes from species like **2**,[1] was also observed (small aromatic resonances can be seen in the spectrum provided as Fig. S3 in the ESI†).

It is notable that following cyclization each geraniol-derived moiety has only one olefin unit for reaction with sulfur, though the possibility of additional crosslinks formed with radicals resulting from allylic H-atom abstraction cannot be ruled out based on the data available. The overall conclusion from the ¹H NMR studies is that cyclic structures contributing to the microstructure **GerS** lead to a lower crosslink density than in the simplistic structures shown in Scheme 2. Although extensive
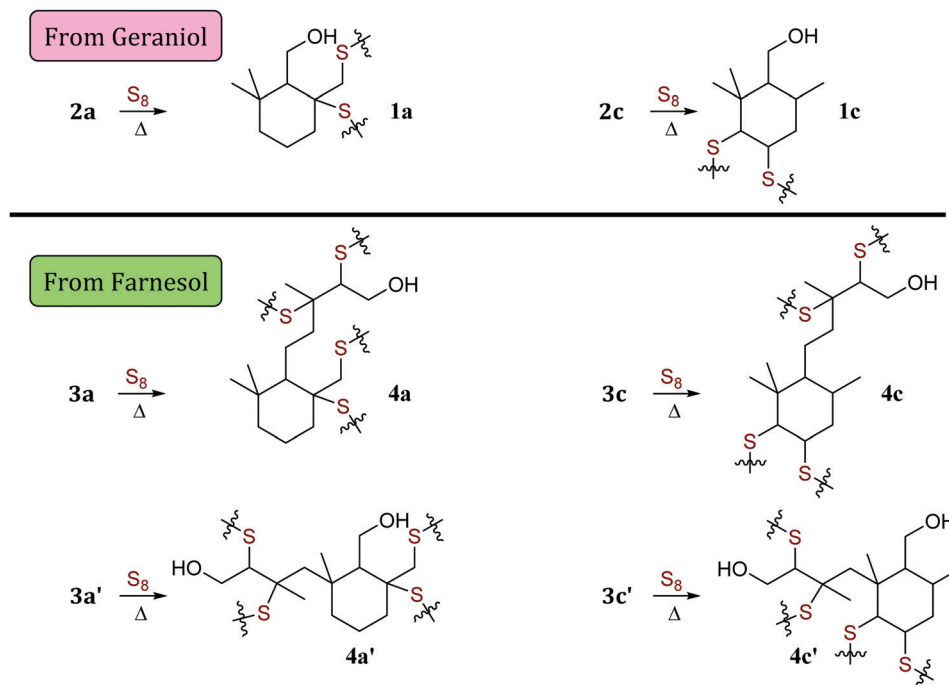
Scheme 4 Microstructures **1** and **4** that result from sulfur crosslinking of olefinic units in species **2** and **3**. Structures of species are summarized in Table 1.

Table 1 Summary of potential cyclization products derived from geraniol (**1** and **2**) or farnesol (**3** and **4**)

Structures	Labels	R		R′	
		–OH	(geranyl –OH)	–CH₃	(geranyl –OH)
2a, 3a, 3a'	**2a**	X		X	
	3a		X	X	
	3a′	X			X
2b, 3b, 3b' (not observed)[a]	**2b**	X		X	
	3b		X	X	
	3b′	X			X
2c, 3c, 3c'	**2c**	X		X	
	3c		X	X	
	3c′	X			X
1d, 4d, 4d'	**1d**	X		X	
	4d		X	X	
	4d′	X			X

[a] Although species **2b**, **3b** and **3b′** can be formed from geraniol and farnesol under some condition, they are not plausible cyclization products under the current conditions and are not observed by ¹H NMR. Downstream structures **1b**, **4b** or **4b′** are not present in **GerS** or **FarS**.

overlap of aliphatic resonances precludes quantification of the extent to which **1a** and **1c** contribute to the structure of **GerS**, integration of observable cyclic olefin precursors suggests a lower limit of 42% for geraniol-derived units in the cyclic form.

The reaction of farnesol with sulfur radicals may be expected to form cyclization products similar to those observed during reaction of geraniol with sulfur. In farnesol, however, either of the two peripheral olefins (starting at C2 or C10) could undergo cyclization upon intramolecular reaction with the more central olefin (Scheme 3B–D). These cyclization reactions would lead to a variety of cyclic products whose structures are summarized in Table 1. Despite the potentially complex mixture of products, efforts were made to observe formation of the cyclic products by ^{1}H NMR analysis of reaction mixtures resulting from the reaction of farnesol with 1, 2, or 4 equivalents of sulfur.

The product mixture resulting from the reaction of farnesol with 1 equivalent of sulfur produced a ^{1}H NMR spectrum (Fig. 3E) similar to that from the analogous reaction with geraniol, producing species attributed to **3a**, **3a′**, **3c** and **3c′**, the analogues of **2a** and **2c**. The ^{1}H NMR spectrum for the reaction mixture resulting from reaction of farnesol with 2 equivalents of sulfur (Fig. 3D) reveals diminishing olefin resonances with concomitant emergence of a peak centred at 3.8 ppm consistent with saturated, sulfur-substituted molecules analogous to species **1**, including **4a**, **4a′**, **4c**, **4c′**, **4d** and **4d′**. Peaks for species **4** continue to increase in intensity as olefin resonances nearly disappear in

the ^{1}H spectrum for the mixture resulting from reaction of farnesol with 4 equivalents of sulfur (Fig. 3C).

A summary of potential microstructures that could result from sulfur crosslinking of the farnesol- and geraniol-derived cyclic olefins is provided in Scheme 4. Although the relative contribution of each particular microstructure to composites **GerS** and **FarS** cannot be quantified from the data presented here due to extensive overlap of resonances, known cyclization products from geraniol and analogous peaks reasonably attributed to farnesol cyclization products are prominent. Efforts are underway to leverage this observation as a potential route to synthesize small molecular terpenoid-derived thiols by their reaction with elemental sulfur, but this work lies outside the scope of the current discussion.

Mechanical properties and possible applications

Having evaluated some microstructural properties of the terpenoid–sulfur composites, it was of interest to assess physical and mechanical properties with an eye towards possible practical applications. The density of the terpenoid–sulfur cements range from 1700–1800 kg m^{-3}, similar to the density of high compressive strength materials like fibre-reinforced resins (*i.e.*, Lyondell Basell product BMC 940-21769) and Portland cement (Table 2), qualifying them as lightweight structural materials by specifications laid out in American Concrete Institute (ACI) standard ACI-213R and ASTM 169C.[66,67]
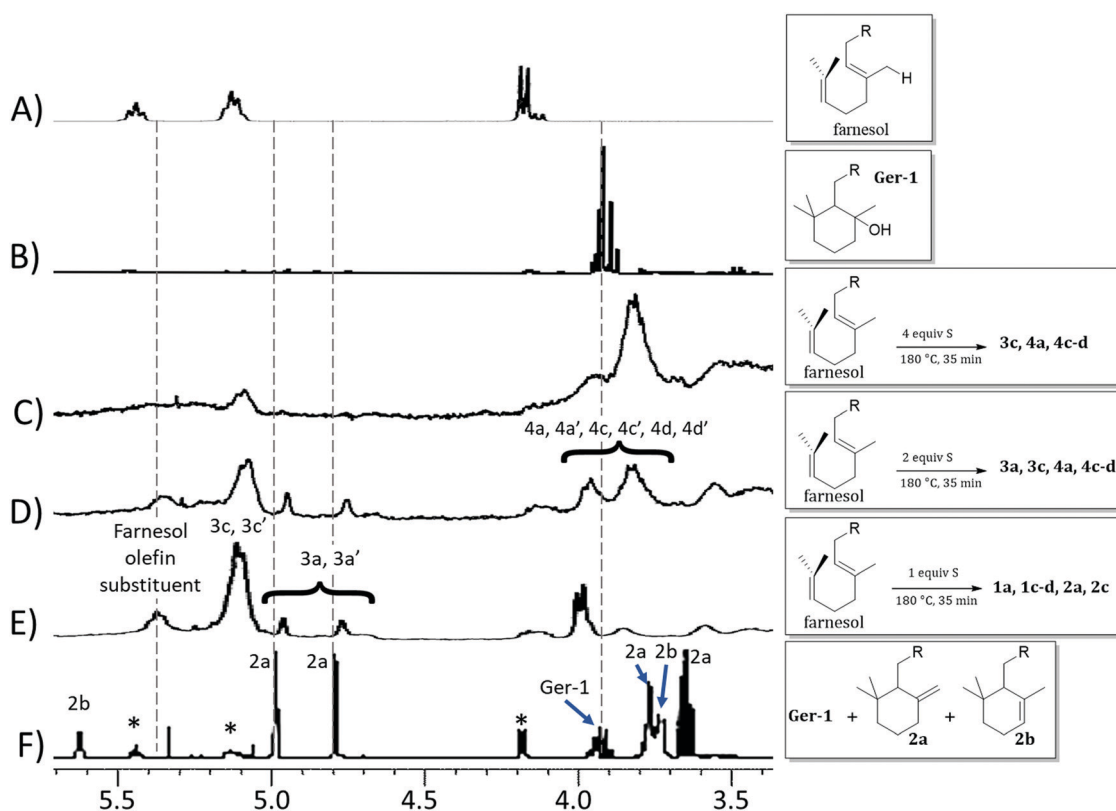

Fig. 3 Proton NMR spectra (CDCl$_3$, 300 MHz) for (A) farnesol, (B) isolated **1b**, and product mixtures resulting from the reaction of farnesol with 4 equiv. S (C), 2 equiv. S (D), or 1 equiv. S (E), and (F) a mixture of geraniol (peaks marked with asterisks), **2a** and **2b**. Spectra (B) and (F) are reprinted from the report,[1] ©20065, with permission from John Wiley and Sons.

Table 2 Physical parameters for plant oil–sulfur composites, Portland cement and composite-infused Portland cement. Each reported value for materials reported herein represents the average of tests on three different samples

	Density (kg m^{-3})	Water uptake (wt%)	Composite uptake (wt%)	Compressive strength	
				As-prepared[a] (% of OCP)	Post-acid retained strength[c] (% of pre-acid)
CitS	1800	0.17	NA	59	80
GerS	1800	0[b]	NA	47	100
FarS	1700	0.12[b]	NA	170	62
BMC 940-21769[d]	1900	<0.10%	NA	206	ND
Portland cement (OPC)	1500	Up to 28%	NA	100[a]	0[e]
CIP	1800	3.2	5.8	110[f]	71[f]
GIP	1900	4.8	9.0	79[f]	60[f]
FIP	1800	5.3	7.3	120[f]	61[f]

[a] Here a value of 17 MPa, the minimum required by ACI 330 for residential building, is used as the compressive strength of OPC. [b] No water uptake within detection limit. [c] Acid challenge involved submersion in 0.5 M H$_2$SO$_4$ for 24 h. [d] A commercial acid-resistant fibre-reinforced vinyl ester resin composite produced by Lyondell Basell for battery and fuel cell components. [e] A sample of OPC deteriorates under these conditions. [f] The compressive strength of the OPC cylinders used to prepare **CIP**, **GIP**, and **FIP** was 19 MPa. The strengths here are expressed as percentages of that original OPC strength.

Water uptake of the materials was assessed as required under ASTM D570 by 24 h submersion at near room temperature. The terpenoid–sulfur composites exhibit very low water uptake (<1%), comparable to organic polymer resins and much lower than the up to 28 wt% water uptake for Portland cement. Low water uptake is an important feature especially for exterior structural applications where water uptake into materials under operational conditions followed by freeze–thaw cycles is a primary cause of fissure formation as absorbed water expands upon freezing, eventually leading to cracked installations and mechanical failure. Low water uptake is also important for maintaining the mechanical integrity of composites, especially bio-derived composites that are often hydrophilic. The tensile strength of polyamide nylon-6,6, for example, drops from 80 MPa to 43 MPa when it absorbs just 3.5 wt% water, which occurs at a relative humidity of just 55%.[68]

Our prior work on high sulfur-content materials suggests a role for them in load-bearing structural applications where high compressive strength is the primary property of interest. The compressive strengths of the three terpenoid–sulfur composites were thus measured for comparison to that of high compressive strength commercial materials. The mechanical strength of previously-reported sulfur–olefin composites generally were shown to increase with increased crosslink density. Among **CitS**, **GerS** and **FarS**, the most-crosslinked **FarS** likewise follows this trend, (Table 2 and Fig. 4; stress–strain plots are provided in Fig. S7, ESI†). In fact, **FarS** exhibits an impressive compressive strength that is 70% higher than required for cement foundations and footings for residential buildings (ACI 332.1R-06). In contrast, **CitS** and **GerS** exhibit much lower compressive strengths of about 30% that shown by **FarS**. The compressive strengths of **CitS** and **GerS** are relatively similar to one another, which is hypothesized to result from significant contribution of cyclic microstructures to **GerS** (*vide supra*).

Previous work on biomolecule-sulfur composites also revealed that such materials can be quite acid resistant.[23,69–73] It was expected that the terpenoid–sulfur composites would likewise be highly resistant to degradation by oxidizing acid. To evaluate their chemical resistance, compressive strength test
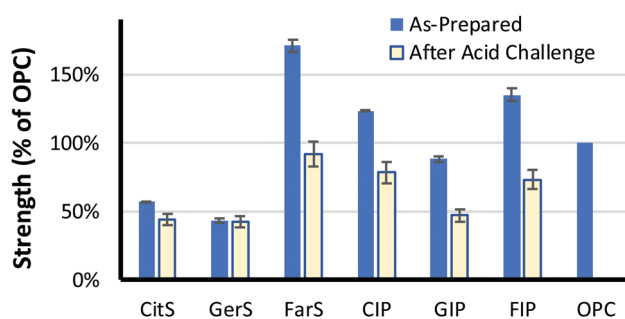

Fig. 4 Compressive strength of terpenoid–sulfur composites (**CitS**, **GerS**, and **FarS**), ordinary Portland cement (OPC) and composite-infused cement (**CIP**, **GIP**, and **FIP**) measures before (blue bars) and after (yellow bars) being submerged in 0.5 M H$_2$SO$_4$ for 24 h. OPC deteriorates after acid challenge so its post-acid strength could not be determined. Each measured value is an average of three trials, and the error bars represent the standard deviation of the three runs.

cylinders of **CitS**, **GerS** and **FarS** were submerged in 0.5 M sulfuric acid for 24 h at 20 °C (Fig. 5A). When a compressive strength test cylinder of the same dimensions made of Portland cement is likewise submerged in 0.5 M sulfuric acid, it disintegrates rapidly, visibly shedding material and changing shape after just 30 minutes (Fig. 5B). In contrast, even over the longer 24 h timescale, the terpenoid–sulfur composites still retain 60–80% of their pre-challenge compressive strength (Table 1 and Fig. 4; stress–strain plots are provided in Fig. S9, ESI†).

Although the low water uptake and acid stability afforded by **CitS**, **GerS** and **FarS** are appealing characteristics for a building material, the low compressive strength of **CitS** and **GerS** compared to Portland cement makes them less attractive in contexts where a very high compressive strength is needed. Despite their low compressive strength on their own, it was hypothesized that these materials could be used as cement additives to enhance the acid resistance and thus the service life of pre-made Portland cement blocks. Compressive strength test cylinders of Portland cement were therefor submerged in molten terpenoid cement and a vacuum was applied for 1 h to pull the molten additive into the pores of the cement following
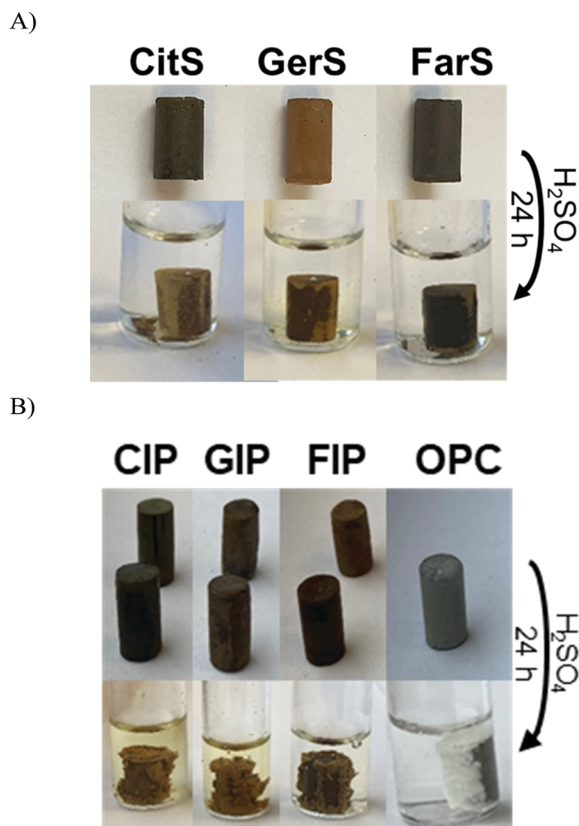
A)

B)

Fig. 5 Appearance of terpenoid–sulfur composite (A) or of ordinary portland cement (OPC) and composite-infused portland cement (B) compressional test cylinders before and after submersion in 0.5 M H_2SO_4 for 24 h.

the reported procedure (photographs of this procedure are provided in the ESI†).[31] After infusing the terpenoid–sulfur cement into the pores by this process, surface polymer was removed and the cylinders were sanded to restore the original cylinder dimensions. This process was repeated with **CitS**, **GerS** and **FarS** to give the infused Portland cements **CIP**, **GIP** and **FIP**, respectively. The amount of terpenoid–sulfur cement taken up by the Portland cement cylinders ranged from 3.2–5.3 wt% (Table 2). While the terpenoid–sulfur composites undergo significant dimensional changes while submerged in the acid, albeit over the much longer timescale than for Portland cement failure, they retain 60–70% of their pre-challenge compressive strength (Table 1 and Fig. 5B).

Conclusions

The characterization of terpenoid–sulfur composites described herein reveals several notable insights. The facile radical-initiated cyclization contributes to the microstructure of **GerS** and **FarS**. Such reactivity should be considered in the analysis of other terpenoid-derived polymers, as the contribution of these structures can have a decided influence on the ultimate physical properties of their composite materials. Composites made by the reaction of terpenoids with sulfur represents a simple and highly atom-economical route to recyclable composites with desirable strength, water uptake, density and chemical resistance metrics competitive with some commercial materials. The terpenoid–sulfur composites can also be used as protectants for mineral cement by their pressure infusion into pre-made cement blocks. The improved understanding of terpenoid polymer microstructures and elucidation of composite materials exhibiting properties on par with established structural materials are important steps towards supplanting traditional materials with greener alternatives.

Experimental

General considerations

Terpenoids (Alfa Aesar or Sigma-Aldrich) and sulfur (Dugas Diesel, USA) were used as received. Portland cement test specimens were prepared by mixing sifted residential Portland cement (Quikcrete, USA) with twice the mass of water and allowing to cure according to manufacturer instructions for residential building purposes. All NMR spectra were recorded on a Bruker Avance spectrometer operating at 300 MHz for protons. Thermogravimetric analysis (TGA) was recorded on a TA SDT Q600 instrument over the range 20 to 800 °C, with a heating rate of 5 °C min^{-1} under a flow of N_2 (100 mL min^{-1}). Differential Scanning Calorimetry (DSC) was acquired using a Mettler Toledo DSC 3 STAR^e System over the range of –50 to 140 °C, with a heating rate of 10 °C min^{-1} under a flow of N_2 (200 mL min^{-1}). Each DSC measurement was carried out over five heat-cool cycles to confirm consistent results following the first heat-cool cycle. The data reported were taken from the third cycle of the experiment. Acid challenge was performed by submerging samples into 0.50 M H_2SO_4 for 24 h after which they were removed, rinsed gently with DI water, and blotted dry.

General reaction of terpenoids with elemental sulfur

Sulfur was melted in a reaction vessel placed in an oil bath at 160 °C with rapid mechanical stirring. The temperature was raised to 180 °C and then the requisite terpenoid was added dropwise to the sulfur. The mixture was rapidly stirred for 35 min at 180 °C and then cooled to room temperature.

CAUTION: Heating elemental sulfur with organics can result in the formation of H_2S gas. The H_2S is toxic, foul-smelling, and corrosive. Although we did not observe any mass loss attributable to gas generation, temperature must be carefully controlled to prevent thermal spikes, which contribute to the potential for H_2S evolution. Rapid stirring, shortened heating times, and very slow addition of reagents can help prevent unforeseen temperature spikes.

Synthesis of CitS

Synthesized according to the general synthesis given above, using citronellol (10.0 g, 64 mmol, d = 0.85 g mL^{-1}) and sulfur (90.1 g, 0.35 mol). Upon cooling to room temperature, the material solidified to a brown solid in quantitative yield. Elemental analysis calcd: C 7.69, H 1.29, S 90.00; found: C 7.77, H 0.98, S 89.39.

Synthesis of GerS

Synthesized according to the general synthesis given above, using geraniol (10.0 g, 65 mmol, 65 mmol, d = 0.89 g mL^{-1}) and

sulfur (90.1 g, 0.35 mol). Upon cooling to room temperature, the material solidified to a brown solid in quantitative yield. Elemental analysis calcd: C 7.79, H 1.18, S 90.00; found: C 7.86, H 0.90, S 89.45.

Synthesis of FarS

Synthesized according to the general synthesis given above, using farnesol (10.0 g, 45 mmol, $d = 0.89$ g mL^{-1}) and sulfur (90.1 g, 0.35 mol). Upon cooling to room temperature, the material solidified to a brown solid in quantitative yield. Elemental analysis calcd: C 8.10, H 1.18, S 90.00; found: C 7.59, H 0.89, S 89.44.

Preparation of CIP, GIP and FIP samples

Impregnation of cement was undertaken by placing a piece of cured Portland cement into a vial of molten terpenoid–sulfur composites submerged in an oil bath at a temperature of 180 °C. Dynamic vacuum was applied for two minutes after which time the vacuum line was closed and a static vacuum was applied for one hour (photographs of this process are provided in the ESI,† Fig. S8). Samples were removed while hot and excess terpenoid–sulfur composite was removed from the surface by sanding to dimensions matching those of the original Portland cement cylinder (±0.05 mm for materials analysed by stress–strain testing).

Compressive strength measurements

Compressive strength tests were acquired using a Mark-10 ES30 Manual Test Stand equipped with a Mark 10 M3-200 Force Gauge (additional details and photographs are provided in the ESI†). terpenoid–sulfur composite materials were aged for 4 d prior to compressive strength testing. The 4 d aging period was selected after assessing material properties over shorter and longer times for one set of samples and the properties were levelled off after 4 d. Longer-term stability is not known for these materials. In many high sulfur-content materials polymeric sulfur domains can revert back to orthorhombic sulfur over longer time spans, with concomitant loss of mechanical properties.

Conflicts of interest

There are no conflicts to declare.

Acknowledgements

Notes and references

1 C. Tsangarakis and M. Stratakis, *Adv. Synth. Catal.*, 2005, **347**, 1280–1284.
2 P. A. Wilbon, F. Chu and C. Tang, *Macromol. Rapid Commun.*, 2013, **34**, 8–37.
3 S. L. Kristufek, K. T. Wacker, Y.-Y. Timothy Tsao, L. Su and K. L. Wooley, *Nat. Prod. Rep.*, 2017, **34**, 433–459.
4 S. Noppalit, A. Simula, N. Ballard, X. Callies, J. M. Asua and L. Billon, *Biomacromolecules*, 2019, **20**, 2241–2251.
5 Y. Zhang, R. S. Glass, K. Char and J. Pyun, *Polym. Chem.*, 2019, **10**, 4078–4105.
6 W. J. Chung, J. J. Griebel, E. T. Kim, H. Yoon, A. G. Simmonds, H. J. Ji, P. T. Dirlam, R. S. Glass, J. J. Wie, N. A. Nguyen, B. W. Guralnick, J. Park, A. Somogyi, P. Theato, M. E. Mackay, Y.-E. Sung, K. Char and J. Pyun, *Nat. Chem.*, 2013, **5**, 518–524.
7 J. M. Chalker, M. J. H. Worthington, N. A. Lundquist and L. J. Esdaile, *Top. Curr. Chem.*, 2019, **377**, 1–27.
8 M. J. H. Worthington, R. L. Kucera and J. M. Chalker, *Green Chem.*, 2017, **19**, 2748–2761.
9 C. Goodyear, *US Pat.*, US3633A, 1844.
10 H. Mutlu, E. B. Ceper, X. Li, J. Yang, W. Dong, M. M. Ozmen and P. Theato, *Macromol. Rapid Commun.*, 2019, **40**, e1800650.
11 S. Oishi, K. Oi, J. Kuwabara, R. Omoda, Y. Aihara, T. Fukuda, T. Takahashi, J.-C. Choi, M. Watanabe and T. Kanbara, *ACS Appl. Polym. Mater.*, 2019, **1**, 1195–1202.
12 D. J. Parker, H. A. Jones, S. Petcher, L. Cervini, J. M. Griffin, R. Akhtar and T. Hasell, *J. Mater. Chem. A*, 2017, **5**, 11682–11692.
13 I. Gomez, O. Leonet, J. A. Blazquez and D. Mecerreyes, *ChemSusChem*, 2016, **9**, 3419–3425.
14 M. P. Crockett, A. M. Evans, M. J. H. Worthington, I. S. Albuquerque, A. D. Slattery, C. T. Gibson, J. A. Campbell, D. A. Lewis, G. J. L. Bernardes and J. M. Chalker, *Angew. Chem., Int. Ed.*, 2016, **55**, 1714–1718.
15 D. J. Parker, S. T. Chong and T. Hasell, *RSC Adv.*, 2018, **8**, 27892–27899.
16 A. D. Tikoalu, N. A. Lundquist and J. M. Chalker, *Adv. Sustainable Syst.*, 2020, **4**, 1900111.
17 M. Mann, J. E. Kruger, F. Andari, J. McErlean, J. R. Gascooke, J. A. Smith, M. J. H. Worthington, C. C. C. McKinley, J. A. Campbell, D. A. Lewis, T. Hasell, M. V. Perkins and J. M. Chalker, *Org. Biomol. Chem.*, 2019, **17**, 1929–1936.
18 M. J. H. Worthington, C. J. Shearer, L. J. Esdaile, J. A. Campbell, C. T. Gibson, S. K. Legg, Y. Yin, N. A. Lundquist, J. R. Gascooke, I. S. Albuquerque, J. G. Shapter, G. G. Andersson, D. A. Lewis, G. J. L. Bernardes and J. M. Chalker, *Adv. Sustainable Syst.*, 2018, **2**, 1800024.
19 N. A. Lundquist, M. J. H. Worthington, N. Adamson, C. T. Gibson, M. R. Johnston, A. V. Ellis and J. M. Chalker, *RSC Adv.*, 2018, **8**, 1232–1236.
20 L. J. Esdaile and J. M. Chalker, *Chem. – Eur. J.*, 2018, **24**, 6905–6916.
21 M. J. H. Worthington, R. L. Kucera, I. S. Albuquerque, C. T. Gibson, A. Sibley, A. D. Slattery, J. A. Campbell, S. F. K. Alboaiji, K. A. Muller, J. Young, N. Adamson, J. R. Gascooke, D. Jampaiah, Y. M. Sabri, S. K. Bhargava, S. J. Ippolito, D. A. Lewis, J. S. Quinton, A. V. Ellis, A. Johs, G. J. L. Bernardes and J. M. Chalker, *Chem. – Eur. J.*, 2017, **23**, 16106.
22 A. Hoefling, Y. J. Lee and P. Theato, *Macromol. Chem. Phys.*, 2017, **218**, 1600303.

23 C. V. Lopez, M. S. Karunarathna, M. K. Lauer, C. P. Maladeniya, T. Thiounn, E. D. Ackley and R. C. Smith, *J. Polym. Sci.*, 2020, **58**, 2259–2266.

24 M. E. Duarte, B. Huber, P. Theato and H. Mutlu, *Polym. Chem.*, 2020, **11**, 241–248.

25 A. D. Smith, R. C. Smith and A. G. Tennyson, *Sustainable Chem. Pharm.*, 2020, **16**, 100249.

26 A. D. Smith, C. D. McMillin, R. C. Smith and A. G. Tennyson, *J. Polym. Sci.*, 2020, **58**, 438–445.

27 A. D. Smith, T. Thiounn, E. W. Lyles, E. K. Kibler, R. C. Smith and A. G. Tennyson, *J. Polym. Sci., Part A: Polym. Chem.*, 2019, **57**, 1704–1710.

28 T. Hasell, P. Yan, W. Zhao, B. Zhang, S. Petcher, A. Smith Jessica, J. Parker Douglas, I. Cooper Andrew, L. Jiang and J. Lei, *Angew. Chem., Int. Ed.*, 2020, **59**, 2–10.

29 T. Thiounn, A. G. Tennyson and R. C. Smith, *RSC Adv.*, 2019, **9**, 31460–31465.

30 A. Hoefling, D. T. Nguyen, Y. J. Lee, S.-W. Song and P. Theato, *Mater. Chem. Front.*, 2017, **1**, 1818–1822.

31 M. K. Lauer, T. A. Estrada-Mendoza, C. D. McMillen, G. Chumanov, A. G. Tennyson and R. C. Smith, *Adv. Sustainable Syst.*, 2019, **3**, 1900062.

32 M. S. Karunarathna, A. G. Tennyson and R. C. Smith, *J. Mater. Chem. A*, 2020, **8**, 548–553.

33 M. S. Karunarathna, M. K. Lauer, T. Thiounn, R. C. Smith and A. G. Tennyson, *J. Mater. Chem. A*, 2019, **7**, 15683–15690.

34 M. S. Karunarathna and R. C. Smith, *Sustainability*, 2020, **12**, 734–748.

35 V. S. Wadi, K. K. Jena, S. Z. Khawaja, V. M. Ranagraj and S. M. Alhassan, *RSC Adv.*, 2019, **9**, 4397–4403.

36 A. M. Abraham, S. V. Kumar and S. M. Alhassan, *Chem. Eng. J.*, 2018, **332**, 1–7.

37 B. Zhang, S. Petcher and T. Hasell, *Chem. Commun.*, 2019, **55**, 10681–10684.

38 C. R. Westerman and C. L. Jenkins, *Macromolecules*, 2018, **51**, 7233–7238.

39 B. Zhang, H. Gao, P. Yan, S. Petcher and T. Hasell, *Mater. Chem. Front.*, 2020, **4**, 669–675.

40 X. Wu, J. A. Smith, S. Petcher, B. Zhang, D. J. Parker, J. M. Griffin and T. Hasell, *Nat. Commun.*, 2019, **10**, 1–9.

41 S. J. Tonkin, C. T. Gibson, J. A. Campbell, D. A. Lewis, A. Karton, T. Hasell and J. M. Chalker, *Chem. Sci.*, 2020, **11**, 5537–5546.

42 N. Lundquist, A. Tikoalu, M. Worthington, R. Shapter, S. Tonkin, F. Stojcevski, M. Mann, C. Gibson, J. Gascooke, A. Karton, L. Henderson, L. Esdaile and J. Chalker, *Chem. – Eur. J.*, 2020, **26**, 1–11.

43 T. Thiounn and R. C. Smith, *J. Polym. Sci.*, 2020, **58**, 1347–1364.

44 M. S. Karunarathna, M. K. Lauer, A. G. Tennyson and R. C. Smith, *Polym. Chem.*, 2020, **11**, 1621–1628.

45 T. Thiounn, M. K. Lauer, M. S. Bedford, R. C. Smith and A. G. Tennyson, *RSC Adv.*, 2018, **8**, 39074–39082.

46 M. Firdaus, L. Montero de Espinosa and M. A. R. Meier, *Macromolecules*, 2011, **44**, 7253–7262.

47 M. Firdaus, *Asian J. Org. Chem.*, 2017, **6**, 1702–1714.

48 J. A. Smith, S. J. Green, S. Petcher, D. J. Parker, B. Zhang, M. J. H. Worthington, X. Wu, C. A. Kelly, T. Baker, C. T. Gibson, J. A. Campbell, D. A. Lewis, M. J. Jenkins, H. Willcock, J. M. Chalker and T. Hasell, *Chem. – Eur. J.*, 2019, **25**, 10433–10440.

49 K. Ohyama, M. Suzuki, J. Kikuchi, K. Saito and T. Muranaka, *Proc. Natl. Acad. Sci. U. S. A.*, 2009, **106**, 725–730.

50 B. G. Bag, A. C. Barai, S. N. Hasan, S. K. Panja, S. Ghorai and S. Patra, *Pure Appl. Chem.*, 2020, **92**, 567–577.

51 C. S. Sell, *A Fragrant Introduction to Terpenoid Chemistry*, 2003.

52 T. K. Devon and A. I. Scott, *Handbood of Naturally Occurring Compounds, Vol. 2: Terpenes*, 1972.

53 W. Templeton, *An Introduction to the Chemistry of the Terpenoids and Steroids*, 1969.

54 *Terpenoids in Plants*, in J. B. Pridham ed. 1967.

55 N. Bauman and I. Ajjawi, *US Pat.*, 2016-US50285, 2017041048, 2017.

56 C. Kempinski, Z. Jiang, S. Bell and J. Chappell, *Adv. Biochem. Eng./Biotechnol.*, 2015, **148**, 161–199.

57 N. Heaps, D. Molina and C. Behnke, *US Pat.*, US26445, 2010104763, 2010.

58 P. Arendt, J. Pollier, N. Callewaert and A. Goossens, *Plant J.*, 2016, **87**, 16–37.

59 L. Putignani, O. Massa and A. Alisi, *Food Res. Int.*, 2013, **54**, 1084–1095.

60 C. Sun, C. Theodoropoulos and S. Scrutton Nigel, *Bioresour. Technol.*, 2020, **300**, 122666.

61 W. Wu and C. T. Maravelias, *Biotechnol. Biofuels*, 2018, **11**, 294.

62 S. C. Hammer, A. Marjanovic, J. M. Dominicus, B. M. Nestl and B. Hauer, *Nat. Chem. Biol.*, 2015, **11**, 121–126.

63 A. M. Arnold, A. Poethig, M. Drees and T. Gulder, *J. Am. Chem. Soc.*, 2018, **140**, 4344–4353.

64 A. Demotie, I. J. S. Fairlamb and S. K. Radford, *Tetrahedron Lett.*, 2003, **44**, 4539–4542.

65 J. M. Janusz, J. M. Gardlik, P. A. Young, R. V. Burkes, S. J. Stoll, A. F. Estelle and C. M. Riley, *J. Med. Chem.*, 1990, **33**, 1052–1061.

66 Lightweight Concrete and Aggregates, Tom Holm, ASTM 169C, ASTM International, West Conshohocken, PA, 2003, ch. 48.

67 American Concrete Institute Committee 213, *A. R. Guide for Structural Lightweight Aggregate Concrete*, Farmington Hills, MI, 1999.

68 C. C. Pai, R. J. Jeng, S. J. Grossman and J. C. Huang, *Adv. Polym. Technol.*, 1989, **9**, 157–163.

69 H. Kwon, A. S. Lee, J. H. Lee, N. K. Park, G. D. Kim, B. Cho, S.-C. Choi and S. Yu, *J. Ind. Eng. Chem.*, 2017, **53**, 386–391.

70 S. Yu, H. Kwon, H. R. Noh, B.-I. Park, N. K. Park, H.-J. Choi, S.-C. Choi and G. D. Kim, *RSC Adv.*, 2015, **5**, 36030–36035.

71 J. Moon, P. D. Kalb, L. Milian and P. A. Northrup, *Cem. Concr. Compos.*, 2016, **67**, 20–29.

72 V. Gupta, S. Ghosh and V. Phapale, *Phosphorus, Sulfur Silicon Relat. Elem.*, 2018, **193**, 752–758.

73 M. Contreras, M. J. Gázquez, I. García-Díaz, F. J. Alguacil, F. A. López and J. P. Bolívar, *J. Environ. Manage.*, 2013, **128**, 625–630.